

# Geophysical Research Letters®



## RESEARCH LETTER

10.1029/2024GL110657

## Plausible Last Interglacial Antarctic Ice Sheet Changes Do Not Fully Explain Antarctic Ice Core Water Isotope Records

### Key Points:

- A compilation of Last Interglacial  $\delta^{18}O$  ice core records shows anomalies of +1.5‰ and +3.3‰ for 127 kyr BP and LIG-peak core-mean
- Simulations run with plausible LIG Antarctic Ice Sheet (AIS) configurations, alongside greenhouse gas and orbital changes, capture < 10% of core-mean differences
- Two LIG AIS configurations yield lower geographical errors at 127 kyr, compared to their PI configurations

### Supporting Information:

Supporting Information may be found in the online version of this article.

### Correspondence to:

H. Zou,  
huiling.zou@vuw.ac.nz

### Citation:

Zou, H., Sime, L. C., Bertler, N. A. N., Keller, E. D., & Wolff, E. W. (2025). Plausible last interglacial Antarctic ice sheet changes do not fully explain Antarctic ice core water isotope records. *Geophysical Research Letters*, 52, e2024GL110657. <https://doi.org/10.1029/2024GL110657>

Received 12 JUN 2024

Accepted 15 DEC 2024

### Author Contributions:

**Conceptualization:** Louise C. Sime

**Data curation:** Huiling Zou

**Funding acquisition:** Louise C. Sime, Nancy A. N. Bertler





**Investigation:** Huiling Zou, Louise C. Sime

**Methodology:** Huiling Zou, Louise C. Sime, Eric W. Wolff

**Supervision:** Louise C. Sime, Nancy A. N. Bertler, Elizabeth D. Keller

**Visualization:** Huiling Zou, Louise C. Sime, Elizabeth D. Keller

**Writing – original draft:** Huiling Zou, Louise C. Sime, Nancy A. N. Bertler

Huiling Zou<sup>1,2,3</sup> , Louise C. Sime<sup>2</sup> , Nancy A. N. Bertler<sup>1,3</sup>, Elizabeth D. Keller<sup>1,3</sup> , and Eric W. Wolff<sup>4</sup> 

<sup>1</sup>Antarctic Research Centre, Victoria University of Wellington, Wellington, New Zealand, <sup>2</sup>British Antarctic Survey, Cambridge, UK, <sup>3</sup>GNS Science, Lower Hutt, New Zealand, <sup>4</sup>Department of Earth Sciences, University of Cambridge, Cambridge, UK

**Abstract** Antarctic ice cores can help determine ice mass loss from the Antarctic Ice Sheet (AIS) during past warm periods. We compile Last Interglacial (LIG)  $\delta^{18}O$  measurements from eight Antarctic cores and compare these to new isotope-enabled LIG simulations, which explore three plausible LIG AIS elevation and extent scenarios. We find that these simulations capture less than 10% of East Antarctic core-mean  $\delta^{18}O$  changes. Although our simulations do not fully explain the changes, they capture some inter-core geographical  $\delta^{18}O$  variations. Some LIG AIS configurations show higher skill than PI AIS configurations in simulating the inter-core differences. The remaining discrepancies between the simulated and observed core-mean water isotope changes suggest that LIG simulations also need to include the influences of reduced Antarctic sea ice, a warmer Southern Ocean, and resultant shifts in vapor source regions to produce a more satisfactory match to  $\delta^{18}O$  observed at ice core sites.

**Plain Language Summary** Reconstructions of Antarctic Ice Sheet (AIS) retreat during past warm periods provide important constraints for projections of future ice mass loss and sea level rise. The Last Interglacial (LIG) is a particularly useful example, when global temperatures were  $1\pm 1^{\circ}C$  warmer than preindustrial (PI) conditions, to explore future sea level rise projections associated with the successful implementation of the Paris Agreement. Here, we use data from six East Antarctic ice cores and two new, unpublished records from West Antarctica that capture LIG conditions. Water isotopes in ice cores are sensitive to changes in temperature, AIS elevation, atmospheric circulation pattern, sea ice area, and ocean conditions. We compare model simulations of the LIG with ice core data and find that elevation changes, an important indicator of ice mass loss, explain only around 9% of the isotope change captured in East Antarctic ice cores. Due to the limitation of our simulations in the coastal regions, our West Antarctic coastal sites are more challenging. In summary, we find that while the range of our simulations does not fully explain average East Antarctic PI-to-LIG isotope changes, they do capture some of the geographical variations in isotope change patterns.

## 1. Introduction

In recent years, West Antarctic Ice Sheet (WAIS) ice mass loss has accelerated in response to ocean warming and changes in ocean circulation (Adusumilli et al., 2020; DeConto & Pollard, 2016; Pollard & DeConto, 2009; Scambos et al., 2017). However, contributions of AIS mass loss to sea level rise remain uncertain (IPCC, 2023; Lhermitte et al., 2020; Rignot et al., 2019; Shepherd et al., 2018). Reconstructions from past warm periods can provide useful constraints to help improve projections of future ice mass loss. A particularly useful example is the Last Interglacial Period (LIG; 116–130 kyr BP) (Masson-Delmotte et al., 2011; Past Interglacials Working Group of PAGES, 2016), when the maximum warming at East Antarctic plateau ice core sites may have reached 3–6°C warmer than preindustrial temperatures (Bakker et al., 2014; Capron et al., 2014; Jouzel et al., 2007; Otto-Bliesner et al., 2013; Sime et al., 2009), and peak LIG global mean sea level (GMSL) was 1.2–8.7 m higher than present (Barnett et al., 2023; Dyer et al., 2021). The deglaciation ice sheet meltwater in the North Atlantic is a key driver of Southern Ocean and Antarctic warming during the LIG (Gao et al., 2024). Given the Greenland Ice Sheet is thought to have contributed 0.7 m (3 m) to GMSL during the LIG in the lowest (highest) melt scenarios (Dumitru et al., 2023), and ocean warming/thermal expansion might have contributed another 0.3–0.7 m (Shackleton et al., 2020), a 1.2–8.7 m GMSL rise requires a contribution of ~0–7.7 m from the AIS (Barnett et al., 2023; Dyer et al., 2021). Ice sheet modeling suggests that AIS loss from the Amundsen sector might have contributed up to

© 2025. The Author(s).

This is an open access article under the terms of the [Creative Commons Attribution License](https://creativecommons.org/licenses/by/4.0/), which permits use, distribution and reproduction in any medium, provided the original work is properly cited.

**Writing – review & editing:** Huiling Zou, Louise C. Sime, Nancy A. N. Bertler, Elizabeth D. Keller, Eric W. Wolff

4 m to GMSL rise during LIG by around 126ky (Clark et al., 2020; Golledge et al., 2021; Lau et al., 2023), whilst there was only a limited LIG retreat of grounded ice in the East Antarctic Wilkes Subglacial Basin region (Crotti et al., 2022; Sutter et al., 2020). Despite these advances, the largest uncertainties surrounding AIS contributions to LIG sea level arise from West Antarctic ice loss.

Antarctic ice cores provide insights into past environmental conditions (EPICA community members, 2004; Fischer et al., 2008; Jouzel et al., 2007; WAIS Divide Project Members, 2015). Ice core stable water isotope ( $\delta^{18}O$ ) values are particularly valuable to investigate past AIS changes because they are sensitive to changes in the hydrological cycle, including condensation temperature, air mass trajectory, and moisture source, all of which are influenced by changes in AIS elevation and extent.

For example, a warmer atmosphere can carry more water vapor, and is usually linked with increased  $\delta^{18}O$ . Moreover, changes in local boundary layer conditions (Krinner et al., 1997), the seasonality of precipitation (Sime et al., 2009), air mass trajectories and vapor-to-precipitation distance (Delaygue et al., 2000; Schlosser et al., 2004), and evaporation and ocean surface conditions (Vimeux et al., 1999), particularly sea ice (Bertler et al., 2018; Holloway et al., 2016, 2017), influence the hydrological cycle. However, the most important control on  $\delta^{18}O$  in polar regions is thought to be condensation temperature, itself strongly dependent on elevation due to lapse-rate effects. Thus site elevation, and its associated condensation (and surface) temperature, is thought to be an overriding control on  $\delta^{18}O$  (Goursaud et al., 2021; Werner et al., 2018). For these reasons, we focus on whether credible LIG changes in AIS, and associated site elevation and temperature changes, can explain Last Interglacial (LIG)  $\delta^{18}O$  values measured in Antarctic ice cores. Previously published ice core records from locations in East Antarctica and two new (unpublished) sites in West Antarctica provide an exciting opportunity to assess possible AIS elevation changes and ice mass loss during the LIG.

To test the most credible AIS elevation change scenarios against ice core data, we set up five LIG isotope-enabled simulations. Isotope enabled climate modeling allows us to investigate whether these scenarios realistically match the observations (Goursaud et al., 2021; Holloway et al., 2016; Werner et al., 2018). Plausible LIG AIS elevation change scenarios are taken from published outputs of dynamic ice sheet model experiments, providing realistic and physically consistent preindustrial (PI) and LIG AIS configurations (Clark et al., 2020; DeConto & Pollard, 2016; Golledge et al., 2021; Pollard & DeConto, 2009).

## 2. Materials and Methods

We describe the LIG Antarctic ice core  $\delta^{18}O$  data and isotopically enabled model simulations used to explore the  $\delta^{18}O$ , SAT and precipitation response to (realistic) plausible LIG ice sheet elevation and extent changes.

### 2.1. Ice Core Data

There are six published East Antarctic ice core records that provide observations from the LIG: Vostok (VK) (Petit et al., 1999); Dome Fuji (DF) (Kawamura et al., 2007); EPICA Dome C (EDC) (Jouzel et al., 2007); EPICA Dronning Maud Land (EDML) (EPICA Community Members, 2006); Talos Dome Ice Core (TALDICE) (Stenni et al., 2011); and Taylor Dome (TD) (Steig et al., 2000).

VK (PI period), DF, and TD are all plotted on the EDC3 chronology (Parrenin et al., 2007), and their  $\delta^{18}O$  records are derived from Masson-Delmotte et al. (2011). The VK (LIG period), EDC, TALDICE, and EDML cores are on the AICC2012 chronology (Bazin et al., 2013; Veres et al., 2013). At 127 ky, EDC3 and AICC2012 differ by less than 0.5 kyr. In addition to these published ice core data, Table 1 contains previously unpublished records from two West Antarctic ice cores: Skytrain (SK), which is missing parts of the LIG, and the Roosevelt Island Climate Evolution project (RICE), which has yet to be robustly dated; both are thought to contain LIG ice.

Our **reference** PI values at each ice core drilling site are an average over 0–2000 years. Ice core  $\delta^{18}O$  values at 127 ky correspond to the average of  $\delta^{18}O$  between 126–127 ky ( $CORE_{127k}$ ), and LIG peak values ( $CORE_{peak}$ ) correspond to the maximum between 120 and 130ky (Figure 1). All raw data are filtered (using a 5 point binomial filter) to represent a 200-year mean before this maximum is calculated. Thus we provide two representative LIG  $\Delta\delta^{18}O$  (PI to LIG) values for each ice core site (“ $CORE_{127k}$ ” and “ $CORE_{peak}$ ”), together with the present day core

**Table 1**

Actual (CORE) and Simulated (DP and PISM) Elevations Alongside Actual and Simulated LIG-PI  $\Delta\delta^{18}O$  ( $DP_{LIG}^{PI}$  Minus  $DP_{PI}^{PI}$ ; and  $PISM_{LIG}^{PI}$  Minus  $PISM_{PI}^{PI}$ ) Values at Eight Ice Core Sites

Core site	Location		Elevation (m)			$\Delta\delta^{18}O$ (‰)			
	Latitude	Longitude	CORE	DP	PISM	CORE <sub>127k</sub>	CORE <sub>peak</sub>	DP	PISM
VK	78° 28' S	108° 48' E	3,488	3,461	3,305	1.4	3.3	0.40	−0.05
DF	77° 19' S	39° 40' E	3,810	3,561	3,467	2.9	4.4	−0.58	−0.10
EDC	75° 06' S	123° 21' E	3,233	3,067	3,022	1.7	4.4	0.16	−0.41
EDML	75° 00' S	00° 04' E	2,882	2,817	2,792	0.9	2.4	−0.16	0.69
TALDICE	72° 49' S	159° 11' E	2,315	2,250	2,136	0.3	3.2	0.33	1.17
TD	77° 47' S	158° 43' E	2,365	2,405	2,531	2	2.1	−1.10	−0.33
RICE	79° 36' S	18° 29' E	550	131	125	—	1.7 <sup>a</sup>	0.93	0.98
SK	79° 44' S	78° 33' W	784	434	731	2.8 <sup>a</sup>	—	1.07	−0.44
SITE MEAN <sup>b</sup>	76' S	98' E	3,016	2,927	2,876	1.53	3.3	−0.16	0.16

Note. For the measured  $\Delta\delta^{18}O$  we provide the value at 127 ky (CORE<sub>127k</sub>) and the LIG maximum (CORE<sub>peak</sub>) value. For SK, the 127 ky value of  $\Delta\delta^{18}O$  is the anomaly between the average value during 125–126ky and PI values of  $\delta^{18}O$ . For RICE, the peak value of  $\Delta\delta^{18}O$  is the anomaly between the likely peak values during the LIG period and PI values of  $\delta^{18}O$ . Since there are no PI to LIG elevation changes between our PI and LIG control simulations, the LIG-PI  $\Delta\delta^{18}O$  simulation anomalies values in the columns headed DP and PISM show only the (simulated) impacts of PI to LIG changes in insolation and GHGs. <sup>a</sup>Confidently dated  $\delta^{18}O$  at 127 ky or LIG maximum not available at this site. For SK, we regard the 125–126 ky mean as the value during the LIG. For RICE, the peak value is considered to be the value in the LIG. <sup>b</sup>Site mean ranges: VK, DF, EDC, EDML, TALDICE, TD.

site elevation (Table 1, “CORE”). The depth-age model for each ice core is described in Text S1 in Supporting Information S1.

## 2.2. Model and Experiments

Simulations are performed using the isotope-enabled ocean-atmosphere coupled general circulation model, HadCM3 (Tindall et al., 2009). The HadCM3 couples a hydrostatic atmospheric component HadAM3 and a barotropic ocean component HadOM3 (details in Text S2 in Supporting Information S1).

We explore the impacts of physically plausible LIG AIS configurations, taking into account LIG climate conditions, using the outputs from published simulations using dynamic ice sheet models. The two ice sheet models used here are the “DP” model from Pollard and DeConto (2009) and DeConto and Pollard (2016), and the PISM model used in Clark et al. (2020) and Golledge et al. (2021). These models use different physics: ice-shelf hydrofracturing and structural collapse of tall, marine-terminating ice cliffs (DP model) and velocity fields from the shallow shelf and shallow ice approximations across the entire domain (PISM model). We therefore set up two reference simulations for the PI. Each of these two PI reference simulations uses the standard PI values for orbital parameters, greenhouse-gas forcing, and solar constant (Otto-Bliesner et al., 2017).

Additionally, we perform simulations that keep elevation and extent unchanged (maintaining the AIS configuration from the PI simulations) but with LIG orbital and GHG forcing. In every case, our LIG simulations use standard PMIP4 LIG values for the 127 ky orbital parameters and GHGs (275 ppm CO<sub>2</sub>, 707 ppb CH<sub>4</sub>, and 266 ppb N<sub>2</sub>O). Because PMIP chose 127 ky as their “Last Interglacial” target for their sets of experiments, a focus on 127 ky is particularly valuable to the paleo community (Kageyama et al., 2018; Yin & Berger, 2010, 2012). For naming convention see Text S3 and Table S1 in Supporting Information S1.

For our main experiment, we perform three LIG simulations, with plausible PI to LIG AIS elevation and extent changes derived from dynamic ice sheet simulations, but no changes to the land-sea mask. These allow us to explore the climate and isotope sensitivity to the impacts of physically plausible LIG AIS changes. Our chosen LIG-specific AIS configurations (Figures 2c–2e) are from Golledge et al. (2021) (Golledge21), Clark et al. (2020) (Clark20), and DeConto and Pollard (2016) (DP16). Each of these LIG simulations is identical to the respective LIG reference simulation to enhance physical consistency (Text S4 in Supporting Information S1), except in the AIS configuration. Thus, assessing the difference between for example, DP16<sup>LIG</sup> and DP16<sup>PI</sup> quantifies the

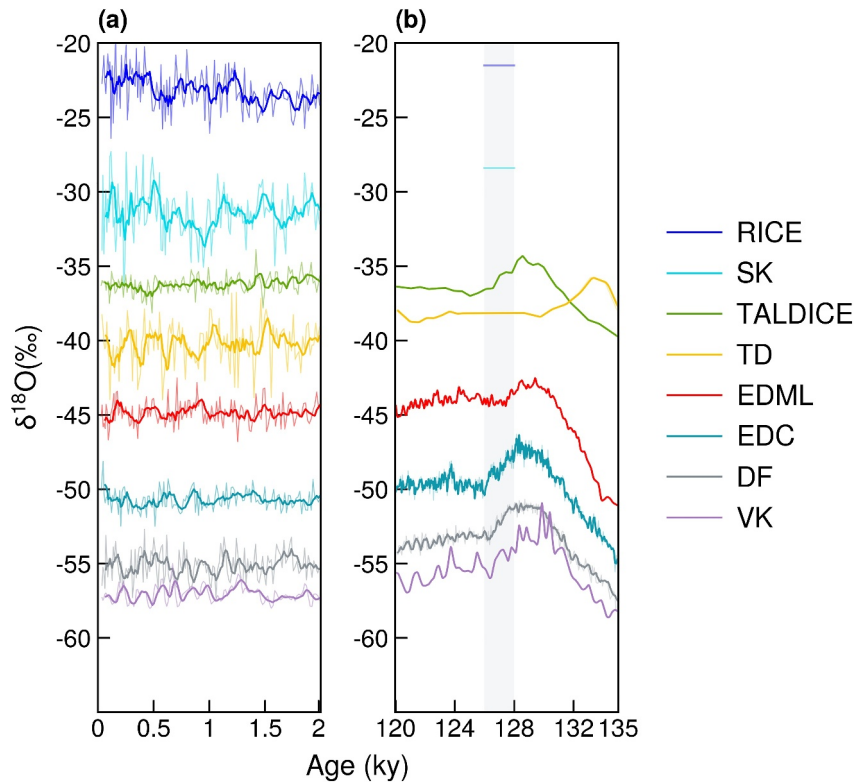


**Figure 1.** Timeseries of water isotope records from six East Antarctic and two West Antarctic ice cores. The figure shows records from the (a) PI period (last 2 ky) and (b) LIG period (135-127 ky). All data sets are set to the AICC2012 age scale. LIG data from SK is only available to 126 ky and is on the ST22 chronology. The RICE section potentially containing LIG data is not yet dated. Instead, we show (unpublished) average values from the section thought to be of LIG age. All raw data (thin lines) are filtered using a 5 point binomial filter to ensure they represent a 200-year mean (bold lines). Shading in panel (b) shows the time period used to calculate average values at 127 ky.

simulated impact of (only) the plausible PI to LIG AIS configuration change (all simulations listed in Table S2 in Supporting Information S1).

Our five AIS configurations (DP, PISM, DP16, Clark20, Golledge21) differ primarily in elevation and extent changes of the WAIS. Note that the Golledge21 and Clark20 AIS configurations are relatively similar; the only difference is the choice of some parameters in PISM: Golledge et al. (2021) modified the mantle viscosity and bed elevation from Clark20 Clark et al. (2020). The DP and DP16 AIS configurations are different from PISM, Golledge21 and Clark20, due to the different physics parameterizations in the ice sheet models (DeConto & Pollard, 2016; Pollard & DeConto, 2009).

All our LIG HadCM3 simulations are integrated for the first 700 years to spin-up, and then run for a further 70 years with each AIS shape. There are no significant trends in the atmosphere, upper and surface ocean during the simulation analysis periods (Goursaud et al., 2021; Holloway et al., 2017). The last 50 years of each simulation are used in our analysis. We focus on  $\Delta$ SAT,  $\Delta$ Precip, and  $\Delta\delta^{18}O$  (LIG - PI changes in surface air temperature, precipitation, and  $\delta^{18}O$ , respectively).

### 2.3. Simulation-Observation Errors

Simulation-observation errors are split into bias error (b), and irreducible error (e):

$$RMSE = \sqrt{\frac{1}{n} \sum_{i=1}^n (y_i - y_i^m)^2} \quad (1)$$

$$b = \sum_{i=1}^n (y_i - y_i^m) / n \quad (2)$$

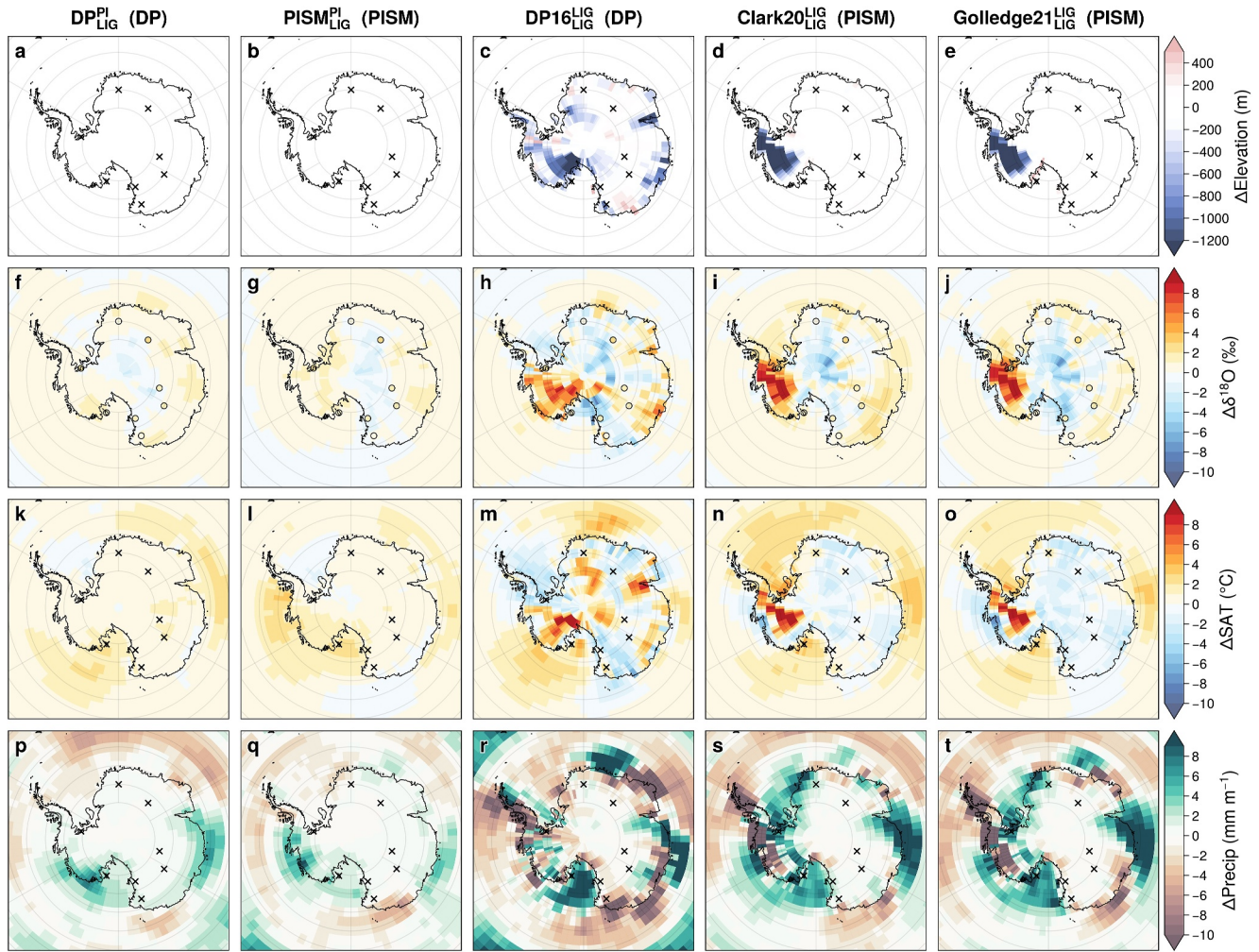


**Figure 2.** Simulated LIG anomalies in  $\delta^{18}O$ , surface air temperature, precipitation and elevation against PI reference simulations ( $DP_{PI}^{PI}$  and  $PISM_{PI}^{PI}$ ). Panels (a–e) are maps of elevation changes (m) in Antarctica relative to PI AIS configurations in DP (against  $DP_{PI}^{PI}$ ), PISM ( $PISM_{PI}^{PI}$ ), DP16 (against  $DP_{PI}^{PI}$ ), Clark20 (against  $PISM_{PI}^{PI}$ ), and Golledge21 (against  $PISM_{PI}^{PI}$ ) scenarios. Panels (f–j) are maps of  $\Delta\delta^{18}O$  (‰) for (f) DP and (h) DP16 against  $DP_{PI}^{PI}$ , (g) PISM, (i) Clark20 and (j) Golledge21 against  $PISM_{PI}^{PI}$ . Panels (k–o) are the same as panels (f–j), but for surface air temperature anomalies ( $^{\circ}C$ ). Panels (p–t) are precipitation anomalies ( $mm\ m^{-1}$ ) for the five scenarios. Each circle in panels (f–j) corresponds to measured LIG-PI  $\Delta\delta^{18}O$  at each ice core site. Black crosses represent ice core locations.

$$e^2 = RMSE^2 - b^2 \quad (3)$$

Where  $y_i^m$  is modeled  $\Delta\delta^{18}O$ ,  $y_i$  is the observed  $\Delta\delta^{18}O$  from ice core measurements.  $n$  is the number of ice cores. This method of error-splitting was first used in Sime and Ferguson (2003).

Statistics for each simulation-observation comparison fit into three cases: (a) all cores; (b) excluding RICE and SK (6 cores); and (c) excluding RICE, SK, and TD (5 cores), the last focusing solely on the AICC2012-dated cores, for both the 127 ky and peak data sets (Tables S4–S6 in Supporting Information S1).

### 3. Results

We examine first the impact of orbital and GHG changes on  $\Delta SAT$ ,  $\Delta Precip$ , and  $\Delta\delta^{18}O$ , and then assess the response to AIS-configuration changes for our AIS scenarios. Finally, we compare the  $\Delta\delta^{18}O$  in the three LIG AIS scenarios with  $\Delta\delta^{18}O$  measured from ice cores.

### 3.1. The Impact of Orbital and GHG Changes

At the LIG, the seasonal cycle in polar regions was stronger than today, with more intense radiative forcing in spring-summer. These spring-summer changes have a large impact on polar climate and hydrology, leading to differences in sea ice, SAT, and precipitation (Diamond et al., 2021; Otto-Bliesner et al., 2021; Sime et al., 2023). The average warming ( $\Delta\text{SAT}$ ) across Antarctica due to orbital and GHGs change in the DP experiments is  $+0.6^\circ\text{C}$  (Figure 2k), and an increase in precipitation ( $\Delta\text{Precip}$ ) across Antarctic of 0.4 mm/month (Figures 2k and 2p). Most of this additional precipitation falls during the colder part of the year.

Despite the warming, the East Antarctic isotopic response to 127 ky orbital and greenhouse gas forcing alone is rather weak, compared to actual ice core values (Figures 2f, 2g, 2k, and 2l): simulated  $\Delta\delta^{18}\text{O}$  values in East Antarctica forced by insolation and GHG changes alone do not match the ice core records. Simulated mean site  $\Delta\delta^{18}\text{O}$  anomalies across East Antarctica are  $-0.16\text{‰}$  and  $+0.16\text{‰}$  for DP and PISM, respectively (simulated individual sites range from  $-1.1\text{‰}$  to  $+1.17\text{‰}$ ), whereas the observed ice core mean values are  $+1.53\text{‰}$  and  $+3.3\text{‰}$  for  $\text{CORE}_{127k}$  and  $\text{CORE}_{\text{peak}}$  (range from  $+0.3\text{‰}$  to  $+4.4\text{‰}$ ) (Table 1).

Holloway et al. (2016) showed that these low modeled  $\Delta\delta^{18}\text{O}$  values (Figures 2f and 2g) are due to changes in both the isotopic composition of precipitation at the ice core site, and an increase in austral winter precipitation in the LIG compared to the PI. While warmer SAT and associated sea-ice retreat can raise  $\delta^{18}\text{O}$  values, the total change in  $\delta^{18}\text{O}$  is only barely positive because of opposing effects from SAT and moisture source distance (positive effects) versus precipitation seasonality (negative effects) (Figures 2k and 2l) (Holloway et al., 2017). Text S5 and Figure S2 in Supporting Information S1 give a quantitative breakdown of these effects. From the PI to LIG, the relative increase in precipitation that falls during colder seasons (Figures S2c and S2d in Supporting Information S1) leads overall to a more depleted  $\delta^{18}\text{O}$  in response to the impact of orbital and GHG changes in some central Antarctic regions (Figures 2f and 2g, blue regions), despite a small warming in these same regions (Figures 2k and 2l). Sea-ice retreat and shorter source-to-site vapor transport pathways raise  $\delta^{18}\text{O}$  values (Figures S2a and S2b in Supporting Information S1). These opposing effects, particularly the precipitation seasonality effect, tend to decouple  $\Delta\delta^{18}\text{O}$  from  $\Delta\text{SAT}$ , resulting in a net simulated near-zero or slightly negative  $\Delta\delta^{18}\text{O}$  across much of East Antarctica. Note, however, that we have used a modern-day fixed-length definition of 12 months with approximately equal season duration in this analysis; with the change in length in months and seasons in the LIG, a seasonal model-data adjustment may be useful (Bartlein & Shafer, 2019). Nevertheless, Figure S1 in Supporting Information S1 show that there are no significant seasonality-related changes to  $\delta^{18}\text{O}$  due to AIS differences.

In West Antarctica, the simulated isotope response is closer to the observations, with the simulated  $\Delta\delta^{18}\text{O} \sim 50\%$  of our quoted (Table 1) CORE  $\Delta\delta^{18}\text{O}$  values. However, we emphasize that the uncertainties on the West Antarctic  $\Delta\delta^{18}\text{O}$  ice core values at RICE and SK are much higher than those from (well-dated) East Antarctica ice cores.

### 3.2. The Impact of LIG AIS Elevation Changes

Given the importance of site temperature, which is largely determined by site elevation, in determining  $\delta^{18}\text{O}$  (Goursaud et al., 2021; Sutter et al., 2020; Werner et al., 2018), it is reasonable to expect a strong imprint of LIG AIS elevation changes on  $\delta^{18}\text{O}$ . However, elevation changes in central East Antarctica in our plausible AIS configurations are relatively small: the mean East Antarctica ice core site  $\Delta\text{Elev}$  values vary between  $-14$  m to  $+49$  m (Table S3 in Supporting Information S1). DP16 shows the highest inter-site variation in ice core site  $\Delta\text{Elev}$ , and the largest East Antarctic mean core site  $\Delta\text{Elev}$  of  $+49$  m. Elevation changes in Clark20 and Golledge21 are smaller. Golledge21 and Clark20 both have substantially higher elevations at SK, and Clark20 at RICE, than DP16.

The HadCM3 modeled responses to three different ice sheet configurations have East Antarctic ice core site-means of:  $\Delta\text{SAT}$  of  $-0.7^\circ\text{C}$ ,  $+0.1^\circ\text{C}$ , and  $-0.5^\circ\text{C}$ ;  $\Delta\text{Precip}$  of  $-0.9$  mm  $\text{m}^{-1}$ ,  $+0.9$  mm  $\text{m}^{-1}$ , and  $+0.4$  mm  $\text{m}^{-1}$ ; and  $\Delta\delta^{18}\text{O}$  of  $-1.1\text{‰}$ ,  $+0.3\text{‰}$ ,  $-0.1\text{‰}$  for the DP16, Clark20, and Golledge21 outputs, respectively. It is interesting to note that using a  $\delta^{18}\text{O}$ -SAT relationship of  $0.8\text{‰}/^\circ\text{C}$  (Markle & Steig, 2022; Masson-Delmotte et al., 2008) to calculate  $\Delta\text{SAT}$  from these  $\Delta\delta^{18}\text{O}$  values, the inferred site-mean warming of these three AIS simulations are  $-1.4^\circ\text{C}$  (actual  $-0.67^\circ\text{C}$ ),  $0.4^\circ\text{C}$  (actual  $0.1^\circ\text{C}$ ), and  $0.1^\circ\text{C}$  (actual  $-0.5^\circ\text{C}$ ), for DP16, Clark20,

and Golledge21 AIS configurations, respectively. Although the actual changes in SAT and  $\delta^{18}O$  are small, the deviation from the expected  $\delta^{18}O$ -SAT relationship is relatively large.

For our West Antarctic coastal sites, modeled  $\Delta\delta^{18}O$  at RICE is  $-1.84\text{‰}$ ,  $-0.21\text{‰}$ , and  $+0.87\text{‰}$  in the DP16, Clark20, and Golledge21 AIS outputs.  $\Delta\delta^{18}O$  at SK are  $+1.93\text{‰}$ ,  $+3.48\text{‰}$ ,  $+5.55\text{‰}$  respectively. At the RICE site, the  $\delta^{18}O$  response to elevation change ( $+17.68$  m) in the Golledge21 scenario is the closest to the measured  $\Delta\delta^{18}O$   $1.7\text{‰}$  in the LIG, but the value ( $0.87\text{‰}$ ) is nearly identical to the  $\Delta\delta^{18}O$   $0.98\text{‰}$  in the PISM<sup>PI</sup><sub>LIG</sub> simulation. At SK, the Clark20 and Golledge21 AIS configurations yield too high  $\Delta\delta^{18}O$  ( $+3.48\text{‰}$  and  $+5.55\text{‰}$ ), almost twice the measured  $\Delta\delta^{18}O$ . Hence, the use of  $\delta^{18}O$  versus elevation relationships ( $\text{‰}/100$  m) previously defined in the literature (Crotti et al., 2022; Sutter et al., 2020; Werner et al., 2018), may cause an under or over estimation of elevation changes, particularly in coastal regions. Given our HadCM3 experiments are conducted at a relatively low resolution, it is difficult to interpret results from coastal regions, as topographic gradients are not well captured in the simulations. For example, high-resolution simulations in a WAIS-collapse scenario (Dütsch et al., 2023) show large changes in atmospheric circulation over West Antarctica, especially at the SK site, which are not well captured by our lower resolution model.

### 3.3. The Simulation of Geographical, or Inter-Core, Differences

Using the Method outlined in Section 2.3, we examine separately simulation-observation bias (b) and irreducible (e) errors. Tables S5 and S6 in Supporting Information S1 show these statistics for each simulation-observation fit in three cases: (a) for all cores; (b) excluding RICE and SK (6 cores); and (c) excluding RICE, SK, and TD (5 cores), focusing solely on the AICC2012-dated cores, for the 127 ky and peak data sets.

The average bias errors (b-values, indicating an offset from the 1:1 measured-modeled line) are 1.5 and 2.9‰, for 127 ky and peak results respectively (Tables S5 and S6 in Supporting Information S1; Figure 3). These values effectively match the 1.6‰ CORE<sub>127k</sub> and 2.9‰ CORE<sub>peak</sub> core-mean measured-modeled offsets. The biases and core-mean values together thus show that the LIG simulations are missing crucial processes and/or changes that are necessary to capture the observed Antarctic ice core LIG  $\Delta\delta^{18}O$  changes that is, some combination of average AIS height and climate errors.

The irreducible error (e-values) indicates geographical mismatches between measured and simulated  $\Delta\delta^{18}O$  values. As such, they are generally attributable to the AIS configuration changes, particularly individual site elevation effects. Therefore, e-values are especially helpful in examining the simulation of geographical, or inter-core, patterns. When considering only the 5 best-dated cores, Golledge21<sup>LIG</sup>, and sometimes DP16<sup>LIG</sup>, generally show the smallest irreducible e-errors, both for 127 ky and for peak core-measurements (Tables S5 and S6 in Supporting Information S1). When either WAIS ice core is included, this is no longer true (Tables S5 and S6 in Supporting Information S1). When looking at peak values, DP16<sup>LIG</sup> and Clark20<sup>LIG</sup> e-values become indistinguishable. Indeed, for peak values, it is also not clear that the LIG AIS shapes are preferable to the PI shapes. DP16<sup>PI</sup><sub>LIG</sub> (a PI AIS configuration) has the second-lowest e-value for the five best-dated cores. This suggests that three LIG AIS shapes might be no better than PI shapes when tested against Antarctic  $\Delta\delta^{18}O$  peak data. Nevertheless, Golledge21<sup>LIG</sup> clearly has the smallest error values related to geographical differences. RMSE, F-values and e-values suggest for the 5 best-dated cores that Golledge21<sup>LIG</sup> and DP16<sup>LIG</sup> are the most accurate at 127 ky. However, given the large (irreducible) b-errors, we emphasize that this study shows that future tests of LIG AIS changes hinge on simulations that better match the warm Southern Ocean and smaller sea ice extent that occurred around 128-127 ky (Gao et al., 2024; Holloway et al., 2016; Sime et al., 2019).

## 4. Discussion and Conclusions

Here we have used three plausible LIG AIS configurations produced by dynamic ice sheet modeling experiments to drive the isotope-enabled model HadCM3 and explore the impact of AIS configuration changes on  $\delta^{18}O$ , SAT, and precipitation in Antarctica during the LIG. Our synthesis of ice core records includes results from two new ice cores located in coastal West Antarctica, SK (Mulvaney et al., 2023) and RICE (Bertler et al., 2018; Lee et al., 2020).

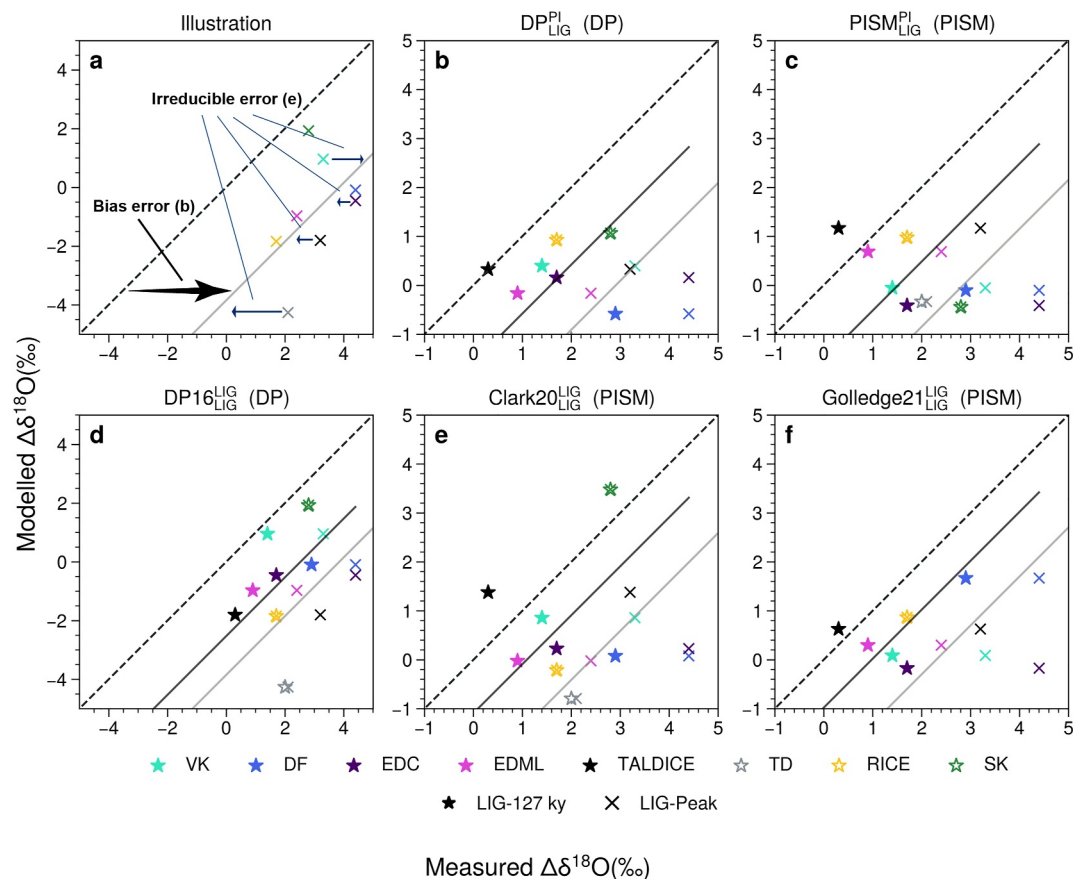


**Figure 3.** Comparison between modeled  $\Delta\delta^{18}O$  (‰) and measured  $\Delta\delta^{18}O$  (‰) in ice cores, relative to 127 ky and LIG peak values. Ice cores shown are Vostok (VK), Dome F (DF), EPICA Dome C (EDC), EPICA Dronning Maud Land (EDML), Talos Dome (TALDICE), Taylor Dome (TD), Roosevelt Island Climate Evolution (RICE), Skytrain (SK). (a) Is an illustrative figure to explain the bias error (b) and irreducible error (e). Comparison between measured  $\Delta\delta^{18}O$  and simulated  $\Delta\delta^{18}O$  from (b)  $DP_{LIG}^{PI}$  (against  $DP_{PI}^{PI}$ ), (c)  $PISM_{LIG}^{PI}$  (against  $PISM_{PI}^{PI}$ ), (d)  $DP16_{LIG}^{LIG}$  (against  $DP_{PI}^{PI}$ ), (e)  $Clark20_{LIG}^{LIG}$  (against  $PISM_{PI}^{PI}$ ), and (f)  $Gollege21_{LIG}^{LIG}$  (against  $PISM_{PI}^{PI}$ ). (b), (c) Show the effects of GHGs forcing and orbital changes. (d–f) Show the combined effects of GHGs forcing, orbital changes, elevation changes. Each star and cross symbol correspond to measured  $\Delta\delta^{18}O$  (‰) in 127 ky and LIG peak values at each site, respectively. Black lines show the 1:1 gradient lines of modeled  $\Delta\delta^{18}O$  and measured  $\Delta\delta^{18}O$  at 127 ky; gray lines show the gradient lines at the LIG peak. The bias errors (b) and irreducible errors (e) for all-core and 6-core (excluding RICE and SK) are shown in Tables S5 and S6 in Supporting Information S1.

Our three LIG AIS configurations show the largest disagreement in ice core site elevation in coastal West Antarctica:  $\Delta Elev$  relative to  $DP^{PI}$  and  $PISM^{PI}$  at RICE (SK) is between  $-100.9$  m and  $+170.1$  m ( $-215.1$  m to  $+176.7$  m). The mean site  $\Delta Elev$  in East Antarctica is comparatively low ( $-13.5$  m to  $+49.3$  m).

By comparing the PI ( $DP_{PI}^{PI}$ ,  $PISM_{PI}^{PI}$ ) and LIG reference simulations ( $DP_{LIG}^{PI}$ ,  $PISM_{LIG}^{PI}$ ), we show that the effects of 127 ky orbital and greenhouse gas forcing on  $\delta^{18}O$  is small. The simulated ice core site mean  $\Delta\delta^{18}O$  in East Antarctica is  $-0.16‰$  using the DP configuration and  $+0.16‰$  using the PISM configuration, while measured site mean  $\Delta\delta^{18}O$  is  $+1.5‰$ . These low and sometimes negative simulated  $\delta^{18}O$  anomalies across East Antarctica do not match the ice core records and indicate that these simulations do not capture the relevant changes which raised  $\delta^{18}O$  during the LIG.

When, in addition to the GHG and orbital changes, we also take into account plausible AIS configurations that capture LIG elevation changes, the discrepancy between the measured and modeled  $\Delta\delta^{18}O$  mean values remains. Modeled site mean  $\Delta\delta^{18}O$  values remain below  $0.3‰$ , which is less than 20% of the measured values ( $1.53‰$ ) at 127 ky (Table 1). Again, this indicates that GHG, orbital and AIS configuration changes alone do not capture the relevant changes in  $\delta^{18}O$ . Despite this, AIS changes do show some agreements with  $\delta^{18}O$  geographical variations,



especially for the Golledge21<sup>LIG</sup> configuration. This AIS configuration has the smallest measured versus modeled geographical errors in  $\delta^{18}O$  at 127 ky and slightly better performance than average for the peak. DP16<sup>LIG</sup> also shows some skill at 127 ky. It is less clear that the three LIG AIS shapes are better than equivalent PI shapes at the peak than at 127 ky; DP16<sup>PI</sup> (a PI configuration) has the second lowest geographical error. LIG AIS configurations thus have some skill at reproducing Antarctic  $\Delta\delta^{18}O$  at 127 ky, but they do not significantly outperform PI configurations when compared to peak data. However, these results comprehensively demonstrate, for the first time, that the influence alone of these four plausible LIG AIS configuration changes on  $\delta^{18}O$  is weak, and thus other factors have important influence.

To explain the most likely PI-to-LIG changes that could have raised  $\delta^{18}O$  and that are missing from these simulations, we turn to the literature. Capron et al. (2017) and Chadwick et al. (2022) showed that mean annual and seasonal Southern Ocean surface temperatures were higher during the LIG, at around 127 ky, compared to the PI. The syntheses in Gao et al. (2024) also support a warmer Southern Ocean and reduced sea ice at 127 ky. Holloway et al. (2016, 2017) demonstrated that the reduction in wintertime Southern Ocean sea ice at 127 ky was important to simulate the correct magnitude of  $\Delta\delta^{18}O$ . Based on these results, Holloway et al. (2018) showed that all these findings could be reconciled if one simulated the Heinrich 11 Northern Hemisphere meltwater-induced bipolar seesaw mechanism. Additionally, Gao et al. (2024) demonstrate that with the simulation of a long (3000 years) Heinrich 11 event at 128 ky, modeled annual and summer SST anomalies are closer to those in the reconstructions at 127 ky. During each deglaciation a substantial volume of fresh water was discharged into the North Atlantic due to the melting of the Laurentide and other Northern Hemisphere ice sheets (Marino et al., 2015). Conditions in the Southern Ocean are closely linked to changes in the North Atlantic; the widely accepted bipolar seesaw concept (Broecker, 1998) explains that deglacial meltwater entering the North Atlantic can reduce ocean convection and the Atlantic Meridional Overturning Circulation (AMOC). This prevents heat from being lost from the global ocean via the North Atlantic and leads to warming in the global and Southern Ocean.

This paper has explored the contribution of plausible AIS changes on Antarctic  $\delta^{18}O$ , and compared the results to ice cores. Through this we have shown, for the first time, that plausible AIS configuration changes, alongside GHG and orbital changes, cannot fully explain the  $\Delta\delta^{18}O$  signals. This most likely means that the impact of the bipolar seesaw, and resultant LIG Southern Ocean warming and sea ice loss, must also be taken into account to explain observed LIG  $\Delta\delta^{18}O$  in Antarctic ice cores.

Future work could tackle this by combining Heinrich-11-induced warming in the Southern Ocean with plausible AIS configuration changes. The 1600-year long Heinrich-11 type simulations of Holloway et al. (2018) do show an Antarctic LIG warming of more than 2°C relative to the PI. Holloway et al. (2018) however also suggest that a very long 3-4000-year Heinrich-11 type event might be required to capture the full magnitude of the LIG warming in Antarctica, a finding backed up by the recent Gao et al. (2024) study. Alongside long Heinrich-11 type simulations that capture the impact of the bipolar seesaw preceding the LIG, the use of higher resolution, isotope-enabled models (Dütsch et al., 2023) may help to improve our understanding of  $\delta^{18}O$ -SAT changes at SK and RICE with an improved representation of coastal elevation changes and complex, local interactions with atmospheric circulation and precipitation in the Weddell Sea and Ross Sea regions. Simulations run with a fully coupled ice sheet model may also be useful to take account of regional trends in surface ocean temperatures as they respond to local ice loss, and the resultant impacts on Antarctic  $\Delta$ SAT and  $\Delta\delta^{18}O$  (Hutchinson et al., 2024); for example, additional AIS meltwater in the Southern Ocean can reduce Antarctic Bottom Water production, with knock-on impacts on regional AIS temperatures (Golledge et al., 2019; Hayes et al., 2014; Hutchinson et al., 2024). Either AIS-coupled and/or high resolution modeling could allow further exploration of whether a collapse of the WAIS might lead to significant ocean and atmospheric circulation anomalies and subsequent precipitation patterns over West Antarctica (Dütsch et al., 2023), which both may be key to resolving how WAIS changes imprint on coastal West Antarctic ice core sites. Higher resolution (ocean sub) model simulations may also improve the simulation of LIG changes in the Weddell Sea and Ross Sea gyres' extent and position (Chadwick et al., 2023). Further exploration of how land/sea boundary changes affect Antarctic results, including influences on ocean circulation and heat distribution, is also warranted. Finally, improved representation of sea ice is likely a requisite to resolve outstanding uncertainties in AIS changes during the LIG from  $\delta^{18}O$  in ice cores.

## Data Availability Statement

Model outputs used in this study are available at Zou et al. (2024). The data sets contain seven simulations including two PI simulations and five LIG simulations. In each data, there are three variables: surface elevation (Orog),  $\delta^{18}O$ , precipitation, and surface air temperature.

## Acknowledgments

HZ, LCS, NANB, and EDK have been funded by the New Zealand Ministry of Business, Innovation and Employment/ Royal Society of New Zealand grants through Victoria University of Wellington (RDF-VUW-1103, 15-VUW-131) and GNS Science (19-GNS-006, Global Change through Time Programme C05X1702). LCS acknowledges additional support from NERC Grant NE/X009386/1; alongside DEEPICE: Understanding Deep Ice Core Proxies to Infer Past Antarctic Climate Dynamics, EU-H2020G.N.955750; ANTSIE: ANTArctic Sea Ice Evolution from a novel biological archive: EU-H2020G.N.864637 and TiPES: Tipping Points in the Earths System: EU-H2020G.N.820970. Production of the data from Skytrain Ice Rise was funded by the European Research Council under the Horizon 2020 research and innovation programme (grant agreement No 742224, WACSWAIN). EW is also supported by a Royal Society Professorship. Open access publishing facilitated by Victoria University of Wellington, as part of the Wiley - Victoria University of Wellington agreement via the Council of Australian University Librarians.

## References

- Adusumilli, S., Fricker, H. A., Medley, B., Padman, L., & Siegfried, M. R. (2020). Interannual variations in meltwater input to the Southern Ocean from Antarctic ice shelves. *Nature Geoscience*, *13*(9), 616–620. <https://doi.org/10.1038/s41561-020-0616-z>
- Bakker, P., Masson-Delmotte, V., Martrat, B., Charbit, S., Renssen, H., Gröger, M., et al. (2014). Temperature trends during the present and last interglacial periods - A multi-model-data comparison. *Quaternary Science Reviews*, *99*, 224–243. <https://doi.org/10.1016/j.quascirev.2014.06.031>
- Barnett, R. L., Austermann, J., Dyer, B., Telfer, M. W., Barlow, N. L., Boulton, S. J., et al. (2023). Constraining the contribution of the Antarctic ice sheet to last interglacial sea level. *Science Advances*, *9*(27), eadf0198. <https://doi.org/10.1126/sciadv.adf0198>
- Bartlein, P. J., & Shafer, S. L. (2019). Paleo calendar-effect adjustments in time-slice and transient climate-model simulations (PaleoCalAdjust v1.0): Impact and strategies for data analysis. *Geoscientific Model Development*, *12*(9), 3889–3913. <https://doi.org/10.5194/gmd-12-3889-2019>
- Bazin, L., Landais, A., Lemieux-Dudon, B., Toyé Mahamadou Kele, H., Veres, D., Parrenin, F., et al. (2013). An optimized multi-proxy, multi-site Antarctic ice and gas orbital chronology (AICC2012): 120–800 ka. *Climate of the Past*, *9*(4), 1715–1731. <https://doi.org/10.5194/cp-9-1715-2013>
- Bertler, N. A., Conway, H., Dahl-Jensen, D., Emanuelsson, D. B., Winstrup, M., Vallenga, P. T., et al. (2018). The Ross Sea Dipole-temperature, snow accumulation and sea ice variability in the Ross Sea region. *Antarctica, over the past 2700 years*, *14*(2), 193–214. <https://doi.org/10.5194/cp-14-193-2018>
- Broecker, W. S. (1998). Paleocirculation during the last deglaciation: A bipolar seesaw? *Paleoceanography*, *13*(2), 119–121. <https://doi.org/10.1029/97PA03707>
- Capron, E., Govin, A., Feng, R., Otto-Bliesner, B. L., & Wolff, E. W. (2017). Critical evaluation of climate syntheses to benchmark CMIP6/PMIP4 127 ka Last Interglacial simulations in the high-latitude regions. *Quaternary Science Reviews*, *168*, 137–150. <https://doi.org/10.1016/j.quascirev.2017.04.019>
- Capron, E., Govin, A., Stone, E. J., Masson-Delmotte, V., Mulitza, S., Otto-Bliesner, B., et al. (2014). Temporal and spatial structure of multi-millennial temperature changes at high latitudes during the Last interglacial. *Quaternary Science Reviews*, *103*, 116–133. <https://doi.org/10.1016/j.quascirev.2014.08.018>
- Chadwick, M., Allen, C. S., Sime, L. C., Crosta, X., & Hillenbrand, C. D. (2022). Reconstructing Antarctic winter sea-ice extent during Marine Isotope Stage 5e. *Climate of the Past*, *18*(1), 129–146. <https://doi.org/10.5194/cp-18-129-2022>
- Chadwick, M., Sime, L. C., Allen, C. S., & Guarino, M. (2023). Model-data comparison of Antarctic winter sea-ice extent and southern ocean sea-surface temperatures during marine isotope stage 5e. *Paleoceanography and Paleoclimatology*, *38*(6), e2022PA004600. <https://doi.org/10.1029/2022pa004600>
- Clark, P. U., He, F., Golledge, N. R., Mitrovica, J. X., Dutton, A., Hoffman, J. S., & Dendy, S. (2020). Oceanic forcing of penultimate deglacial and last interglacial sea-level rise. *Nature*, *577*(7792), 660–664. <https://doi.org/10.1038/s41586-020-1931-7>
- Crotti, I., Quiquet, A., Landais, A., Stenni, B., Wilson, D. J., Severi, M., et al. (2022). Wilkes subglacial basin ice sheet response to Southern Ocean warming during late Pleistocene interglacials. *Nature Communications*, *13*(1), 5328. <https://doi.org/10.1038/s41467-022-32847-3>
- DeConto, R. M., & Pollard, D. (2016). Contribution of Antarctica to past and future sea-level rise. *Nature*, *531*(7596), 591–597. <https://doi.org/10.1038/nature17145>
- Delaygue, G., Jouzel, J., Masson, V., Koster, R. D., & Bard, E. (2000). Validity of the isotopic thermometer in central Antarctica: Limited impact of glacial precipitation seasonality and moisture origin. *Geophysical Research Letters*, *27*(17), 2677–2680. <https://doi.org/10.1029/2000GL011530>
- Diamond, R., Sime, L. C., Schroeder, D., & Guarino, M. V. (2021). The contribution of melt ponds to enhanced Arctic sea-ice melt during the Last Interglacial. *The Cryosphere*, *15*(11), 5099–5114. <https://doi.org/10.5194/tc-15-5099-2021>
- Dumitru, O. A., Dyer, B., Austermann, J., Sandstrom, M. R., Goldstein, S. L., D'Andrea, W. J., et al. (2023). Last interglacial global mean sea level from high-precision U-series ages of Bahamian fossil coral reefs. *Quaternary Science Reviews*, *318*, 108287. <https://doi.org/10.1016/j.quascirev.2023.108287>
- Dütsch, M., Steig, E. J., Blossey, P. N., & Pauling, A. G. (2023). Response of water isotopes in precipitation to a collapse of the West Antarctic ice sheet in high-resolution simulations with the weather research and forecasting model. *Journal of Climate*, *36*(16), 5417–5430. <https://doi.org/10.1175/jcli-d-22-0647.1>
- Dyer, B., Austermann, J., D'Andrea, W. J., Creel, R. C., Sandstrom, M. R., Cashman, M., et al. (2021). Sea-level trends across the Bahamas constrain peak last interglacial ice melt. *Proceedings of the National Academy of Sciences of the United States of America*, *118*(33), e2026839118. <https://doi.org/10.1073/pnas.2026839118>
- EPICA community members. (2004). Eight glacial cycles from an Antarctic ice core. *Nature*, *429*(6992), 623–628. <https://doi.org/10.1038/nature02599>
- EPICA Community Members. (2006). One-to-one coupling of glacial climate variability in Greenland and Antarctica. *Nature*, *444*(7116), 195–198. <https://doi.org/10.1038/nature05301>
- Fischer, H., Behrens, M., Bock, M., Richter, U., Schmitt, J., Loulergue, L., et al. (2008). Changing boreal methane sources and constant biomass burning during the last termination. *Nature*, *452*(7189), 864–867. <https://doi.org/10.1038/nature06825>
- Gao, Q., Capron, E., Sime, L. C., Rhodes, R. H., Sivankutty, R., Zhang, X., et al. (2024). Assessment of the southern polar and subpolar warming in the PMP4 Last Interglacial simulations using paleoclimate data syntheses. *EGU Sphere*, 1–32. <https://doi.org/10.5194/egusphere-2024-1261>
- Golledge, N. R., Clark, P. U., He, F., Dutton, A., Turney, C. S., Fogwill, C. J., et al. (2021). Retreat of the Antarctic ice sheet during the last interglaciation and implications for future change. *Geophysical Research Letters*, *48*(17), e2021GL094513. <https://doi.org/10.1029/2021GL094513>
- Golledge, N. R., Keller, E. D., Gomez, N., Naughten, K. A., Bernales, J., Trusel, L. D., & Edwards, T. L. (2019). Global environmental consequences of twenty-first-century ice-sheet melt. *Nature*, *566*(7742), 65–72. <https://doi.org/10.1038/s41586-019-0889-9>

- Goursaud, S., Holloway, M., Sime, L., Wolff, E., Valdes, P., Steig, E. J., & Pauling, A. (2021). Antarctic ice sheet elevation impacts on water isotope records during the last interglacial. *Geophysical Research Letters*, *48*(6), e2020GL091412. <https://doi.org/10.1029/2020GL091412>
- Hayes, C. T., Martínez-García, A., Hasenfratz, A. P., Jaccard, S. L., Hodell, D. A., Sigman, D. M., et al. (2014). A stagnation event in the deep south atlantic during the last interglacial period. *Science*, *346*(6216), 1514–1517. <https://doi.org/10.1126/science.1256620>
- Holloway, M. D., Sime, L. C., Allen, C. S., Hillenbrand, C. D., Bunch, P., Wolff, E., & Valdes, P. J. (2017). The spatial structure of the 128 ka Antarctic Sea Ice minimum. *Geophysical Research Letters*, *44*(21), 11129–11139. <https://doi.org/10.1002/2017GL074594>
- Holloway, M. D., Sime, L. C., Singarayer, J. S., Tindall, J. C., Bunch, P., & Valdes, P. J. (2016). Antarctic last interglacial isotope peak in response to sea ice retreat not ice-sheet collapse. *Nature Communications*, *7*(1), 12293. <https://doi.org/10.1038/ncomms12293>
- Holloway, M. D., Sime, L. C., Singarayer, J. S., Tindall, J. C., & Valdes, P. J. (2018). Simulating the 128-ka Antarctic climate response to northern Hemisphere ice sheet melting using the isotope-enabled HadCM3. *Geophysical Research Letters*, *45*(21), 11921–11929. <https://doi.org/10.1029/2018GL079647>
- Hutchinson, D. K., Menviel, L., Meissner, K. J., & Hogg, A. M. C. (2024). East Antarctic warming forced by ice loss during the Last Interglacial. *Nature Communications*, *15*(1), 1026. <https://doi.org/10.1038/s41467-024-45501-x>
- IPCC. (2023). Technical summary. In *Climate change 2021 – the physical science basis*. <https://doi.org/10.1017/9781009157896.002>
- Jouzel, J., Masson-Delmotte, V., Cattani, O., Dreyfus, G., Falourd, S., Hoffmann, G., et al. (2007). Orbital and millennial antarctic climate variability over the past 800,000 years. *Science*, *317*(5839), 793–796. <https://doi.org/10.1126/science.1141038>
- Kageyama, M., Braconnot, P., Harrison, S. P., Haywood, A. M., JungCLAUS, J. H., Otto-Bliesner, B. L., et al. (2018). The PMIP4 contribution to CMIP6 - Part 1: Overview and over-arching analysis plan. *Geoscientific Model Development*, *11*(3), 1033–1057. <https://doi.org/10.5194/gmd-11-1033-2018>
- Kawamura, K., Parrenin, F., Lisiecki, L., Uemura, R., Vimeux, F., Severinghaus, J. P., et al. (2007). Northern Hemisphere forcing of climatic cycles in Antarctica over the past 360,000 years. *Nature*, *448*(7156), 912–916. <https://doi.org/10.1038/nature06015>
- Krinner, G., Genthon, C., & Jouzel, J. (1997). GCM analysis of local influences on ice core  $\delta$  signals. *Geophysical Research Letters*, *24*(22), 2825–2828. <https://doi.org/10.1029/97GL52891>
- Lau, S. C., Wilson, N. G., Golledge, N. R., Naish, T. R., Watts, P. C., Silva, C. N., et al. (2023). Genomic evidence for West Antarctic ice sheet collapse during the last interglacial. *Science*, *382*(6677), 1384–1389. <https://doi.org/10.1126/science.ade0664>
- Lee, J. E., Brook, E. J., Bertler, N. A., Buizert, C., Baisden, T., Blunier, T., et al. (2020). An 83 000-year-old ice core from Roosevelt Island, Ross Sea, Antarctica. *Climate of the Past*, *16*(5), 1691–1713. <https://doi.org/10.5194/cp-16-1691-2020>
- Lhermitte, S., Sun, S., Shuman, C., Wouters, B., Pattyn, F., Wuite, J., et al. (2020). Damage accelerates ice shelf instability and mass loss in Amundsen Sea Embayment. *Proceedings of the National Academy of Sciences of the United States of America*, *117*(40), 24735–24741. <https://doi.org/10.1073/pnas.1912890117>
- Marino, G., Rohling, E. J., Rodríguez-Sanz, L., Grant, K. M., Heslop, D., Roberts, A. P., et al. (2015). Bipolar seesaw control on last interglacial sea level. *Nature*, *522*(7555), 197–201. <https://doi.org/10.1038/nature14499>
- Markle, B. R., & Steig, E. J. (2022). Improving temperature reconstructions from ice-core water-isotope records. *Climate of the Past*, *18*(6), 1321–1368. <https://doi.org/10.5194/cp-18-1321-2022>
- Masson-Delmotte, V., Buiron, D., Ekaykin, A., Frezzotti, M., Gallée, H., Jouzel, J., et al. (2011). A comparison of the present and last interglacial periods in six Antarctic ice cores. *Climate of the Past*, *7*(2), 397–423. <https://doi.org/10.5194/cp-7-397-2011>
- Masson-Delmotte, V., Hou, S., Ekaykin, A., Jouzel, J., Aristarain, A., Bernardo, R. T., et al. (2008). A review of antarctic surface snow isotopic composition: Observations, atmospheric circulation, and isotopic modeling. *Journal of Climate*, *21*(13), 3359–3387. <https://doi.org/10.1175/2007JCLI2139.1>
- Mulvaney, R., Wolff, E. W., Grieman, M. M., Hoffmann, H. H., Humby, J. D., Nehrbass-Ahles, C., et al. (2023). The ST22 chronology for the Skytrain Ice Rise ice core - Part 2: An age model to the last interglacial and disturbed deep stratigraphy. *Climate of the Past*, *19*(4), 851–864. <https://doi.org/10.5194/cp-19-851-2023>
- Otto-Bliesner, B. L., Braconnot, P., Harrison, S. P., Lunt, D. J., Abe-Ouchi, A., Albani, S., et al. (2017). The PMIP4 contribution to CMIP6 - Part 2: Two interglacials, scientific objective and experimental design for Holocene and Last Interglacial simulations. *Geoscientific Model Development*, *10*(11), 3979–4003. <https://doi.org/10.5194/gmd-10-3979-2017>
- Otto-Bliesner, B. L., Brady, E. C., Zhao, A., Brierley, C. M., Axford, Y., Capron, E., et al. (2021). Large-scale features of last interglacial climate: Results from evaluating the lig127k simulations for the coupled model intercomparison project (CMIP6)-Paleoclimate modeling intercomparison project (PMIP4). *Climate of the Past*, *17*(1), 63–94. <https://doi.org/10.5194/cp-17-63-2021>
- Otto-Bliesner, B. L., Rosenbloom, N., Stone, E. J., McKay, N. P., Lunt, D. J., Brady, E. C., & Overpeck, J. T. (2013). How warm was the last interglacial? New model-data comparisons. *Philosophical Transactions of the Royal Society A: Mathematical, Physical & Engineering Sciences*, *371*(2001), 20130097. <https://doi.org/10.1098/rsta.2013.0097>
- Parrenin, F., Barnola, J. M., Beer, J., Blunier, T., Castellano, E., Chappellaz, J., et al. (2007). The EDC3 chronology for the EPICA Dome C ice core. *Climate of the Past*, *3*(3), 485–497. <https://doi.org/10.5194/cp-3-485-2007>
- Past Interglacials Working Group of PAGES. (2016). Interglacials of the last 800,000 years. *Reviews of Geophysics*, *54*(1), 162–219. <https://doi.org/10.1002/2015RG000482>
- Petit, J. R., Raynaud, D., Basile, I., Chappellaz, J., Davisk, M., Ritz, C., et al. (1999). Climate and atmospheric history of the past 420, 000 years from the Vostok ice core, Antarctica. *Nature*, *399*(6735), 429–436. <https://doi.org/10.1038/20859>
- Pollard, D., & DeConto, R. M. (2009). Modelling West Antarctic ice sheet growth and collapse through the past five million years. *Nature*, *458*(7236), 329–332. <https://doi.org/10.1038/nature07809>
- Rignot, E., Mouginot, J., Scheuchl, B., Van Den Broeke, M., Van Wessem, M. J., & Morlighem, M. (2019). Four decades of Antarctic ice sheet mass balance from 1979–2017. *Proceedings of the National Academy of Sciences*, *116*(4), 1095–1103. <https://doi.org/10.1073/pnas.1812883116>
- Scambos, T. A., Bell, R. E., Alley, R. B., Anandakrishnan, S., Bromwich, D. H., Brunt, K., et al. (2017). How much, how fast? A science review and outlook for research on the instability of Antarctica's Thwaites Glacier in the 21st century. *Global and Planetary Change*, *153*, 16–34. <https://doi.org/10.1016/j.gloplacha.2017.04.008>
- Schlosser, E., Reijmer, C., Oerter, H., & Graf, W. (2004). The influence of precipitation origin on the  $\delta^{18}O$ -T relationship at Neumayer station, Ekströmsisen, Antarctica. *Annals of Glaciology*, *39*, 41–48. <https://doi.org/10.3189/172756404781814276>
- Shackleton, S., Baggenstos, D., Menking, J. A., Dyonisius, M. N., Bereiter, B., Bauska, T. K., et al. (2020). Global ocean heat content in the Last Interglacial. *Nature Geoscience*, *13*(1), 77–81. <https://doi.org/10.1038/s41561-019-0498-0>
- Shepherd, A., Fricker, H. A., & Farrell, S. L. (2018). Trends and connections across the Antarctic cryosphere. *Nature*, *558*(7709), 223–232. <https://doi.org/10.1038/s41586-018-0171-6>

- Sime, L. C., Carlson, A. E., & Holloway, M. D. (2019). On recovering Last Interglacial changes in the Antarctic ice sheet. *Past Global Changes Magazine*, 27(1), 14–15. <https://doi.org/10.22498/pages.27.1.14>
- Sime, L. C., & Ferguson, R. I. (2003). Information on grain sizes in gravel-bed rivers by automated image analysis. *Journal of Sedimentary Research*, 73(4), 630–636. <https://doi.org/10.1306/112102730630>
- Sime, L. C., Sivankutty, R., Vallet-Malmierca, I., De Boer, A. M., & Sicard, M. (2023). Summer surface air temperature proxies point to near-sea-ice-free conditions in the Arctic at 127 ka. *Climate of the Past*, 19(4), 883–900. <https://doi.org/10.5194/cp-19-883-2023>
- Sime, L. C., Wolff, E. W., Oliver, K. I., & Tindall, J. C. (2009). Evidence for warmer interglacials in East Antarctic ice cores. *Nature*, 462(7271), 342–345. <https://doi.org/10.1038/nature08564>
- Steig, E. J., Morse, D. L., Waddington, E. D., Stuiver, M., Grootes, P. M., Mayewski, P. A., et al. (2000). Wisconsinan and holocene climate history from an ice core at Taylor Dome, western Ross embayment, Antarctica. *Geografiska Annaler - Series A: Physical Geography*, 82(2–3), 213–235. <https://doi.org/10.1111/1468-0459.00122>
- Stenni, B., Buiron, D., Frezzotti, M., Albani, S., Barbante, C., Bard, E., et al. (2011). Expression of the bipolar see-saw in Antarctic climate records during the last deglaciation. *Nature Geoscience*, 4(1), 46–49. <https://doi.org/10.1038/ngeo1026>
- Sutter, J., Eisen, O., Werner, M., Grosfeld, K., Kleiner, T., & Fischer, H. (2020). Limited retreat of the Wilkes basin ice sheet during the last interglacial. *Geophysical Research Letters*, 47(13), e2020GL088131. <https://doi.org/10.1029/2020GL088131>
- Tindall, J. C., Valdes, P. J., & Sime, L. C. (2009). Stable water isotopes in HadCM3: Isotopic signature of El Niño–Southern Oscillation and the tropical amount effect. *Journal of Geophysical Research*, 114(4), D04111. <https://doi.org/10.1029/2008JD010825>
- Veres, D., Bazin, L., Landais, A., Toyé Mahamadou Kele, H., Lemieux-Dudon, B., Parrenin, F., et al. (2013). The Antarctic ice core chronology (AICC2012): An optimized multi-parameter and multi-site dating approach for the last 120 thousand years. *Climate of the Past*, 9(4), 1733–1748. <https://doi.org/10.5194/cp-9-1733-2013>
- Vimeux, F., Masson, V., Jouzel, J., Stievenard, M., & Petit, J. R. (1999). Glacial-interglacial changes in ocean surface conditions in the Southern Hemisphere. *Nature*, 398(6726), 410–413. <https://doi.org/10.1038/18860>
- WAIS Divide Project Members. (2015). Precise interglacial phasing of abrupt climate change during the last ice age. *Nature*, 520(7549), 661–665. <https://doi.org/10.1038/nature14401>
- Werner, M., Jouzel, J., Masson-Delmotte, V., & Lohmann, G. (2018). Reconciling glacial Antarctic water stable isotopes with ice sheet topography and the isotopic paleothermometer. *Nature Communications*, 9(1), 3537. <https://doi.org/10.1038/s41467-018-05430-y>
- Yin, Q. Z., & Berger, A. (2010). Insolation and CO<sub>2</sub> contribution to the interglacial climate before and after the Mid-Brunhes Event. *Nature Geoscience*, 3(4), 243–246. <https://doi.org/10.1038/ngeo771>
- Yin, Q. Z., & Berger, A. (2012). Individual contribution of insolation and CO<sub>2</sub> to the interglacial climates of the past 800,000 years. *Climate Dynamics*, 38(3–4), 709–724. <https://doi.org/10.1007/s00382-011-1013-5>
- Zou, H., Sime, L., Bertler, N., Elizabeth, D. K., & Wolff, E. (2024). Plausible Last Interglacial Antarctic ice sheet changes do not fully explain Antarctic ice core water isotope records [Dataset]. *Zenodo*. <https://doi.org/10.5281/zenodo.13559668>